Journal of Advanced Marine Engineering and Technology, Vol. 49, No. 4, pp. 262~268, 2025
J. Advanced Marine Engineering and Technology (JAMET)
https://doi.org/10.5916/jamet.2025.49.4.262

ISSN 2234-7925 (Print)
ISSN 2765-4796 (Online)
Original Paper

A study on the effects of crescent-shaped wing sails on ship propulsion performance

Jeong-Hwan Kim†

(Received July 22, 2025； Revised August 5, 2025； Accepted August 21, 2025)

Abstract: This study entailed an analysis of the aerodynamic performance of wing sails with crescent-shaped airfoils by using computational fluid dynamics (CFD). Owing to recent International Maritime Organization environmental regulations, wind-assisted propulsion technologies have gained attention, with wing sails being particularly promising because of their simple structure and high propulsion efficiency. Although crescent-shaped designs generate strong lift, studies on the impact of geometric variations remain limited. Therefore, this study evaluated the thrust coefficients (Ct) for six configurations combining three thickness levels (T10, T20, and T30) and two camber values (C10 and C20) under omnidirectional wind conditions ranging from 0° to 360°. The results were visualized using polar plots. The T10_C20 and T30_C10 configurations yielded the highest and lowest thrusts, respectively. These findings offer valuable design guidance for optimizing crescent-shaped wing sails.

Keywords: Wind-Assisted Propulsion, Aerodynamic Performance, Computational Fluid Dynamics, Thrust Coefficient, IMO(International Maritime Organization), Wing Sail

1. Introduction

Given the global climate crisis, the International Maritime Organization (IMO) has implemented a series of environmental regulations aimed at reducing greenhouse gas (GHG) emissions from the shipping industry. As maritime transport accounts for approximately 90% of global trade volume, it plays a crucial role in international logistics. However, the environmental impact of the sector has become increasingly significant, prompting strong calls for enhanced regulatory frameworks. In response, the IMO has set ambitious targets—improving ship energy efficiency by at least 40% by 2030 compared with 2008 levels and reducing total GHG emissions by 50% by 2050 **[1][2]**. To achieve these goals, it has introduced quantitative measures such as the Energy Efficiency Existing Ship Index and the Carbon Intensity Indicator, which monitor and manage ship fuel consumption and carbon emissions annually **[3][4]**. These regulatory efforts have driven major technological innovations and operational shifts across ship design, propulsion systems, and voyage planning **[5]**.

Among the various technologies, wind-assisted propulsion systems have emerged as promising and eco-friendly **[6]**. These systems harness wind power to simultaneously reduce fuel consumption and carbon emissions, thereby supporting regulatory compliance and promoting environmental sustainability. Technologies such as rotor sails and wing sails are notable examples, as they can be used in conjunction with traditional engine-driven propulsion to enhance overall efficiency **[7][8][9]**.

Wing sails offer significant aerodynamic advantages owing to their fixed wing structure, simplified mechanical design, and high lift-generation capacity **[10]**. Additionally, when combined with autonomous control systems, they can be optimized in real time based on wind direction, wind speed, and vessel routing, enabling adaptability across a wide range of ship types and operational conditions **[11]**.

Recent studies have focused on refining wing sail geometries to maximize performance under diverse maritime conditions **[12]**. Innovative shapes, including symmetric and asymmetric profiles, compound curves, and multi-element designs, have been proposed to improve aerodynamic behavior. Among these, crescent-shaped wing sails have shown promising results owing to their ability to generate high lift coefficients and delay flow separation. Its asymmetric curvature and streamlined tip design suppress vortex formation and broaden the effective angle of attack, ultimately enhancing the propulsion performance **[13]**.

† Corresponding Author (ORCID: http://orcid.org/0009-0002-0506-4620): Chief Researcher, Department of Advanced Performance Technology Headquarters, Korea Marine Equipment Research Institute, 3F, 8, Daepyeongnam-ro, Yeongdo-gu, Busan 49043, Korea, E-mail: jhkim@komeri.re.kr, Tel: 051-417-7097

However, current research on crescent-shaped wing sails is still in the early stages. Computational fluid dynamics (CFD)-based simulations and experimental validations are limited, and systematic design standards and empirical data to support commercialization are lacking. Furthermore, the dynamic nature of marine environments necessitates a thorough analysis of aerodynamic sensitivity and operational stability under varying conditions.

Therefore, this study aimed to investigate the aerodynamic performance of crescent-shaped wing sails using CFD. By examining different geometric configurations, this study sought to quantify the relationship between design parameters and propulsion efficiency. The findings are expected to provide foundational data for shape optimization, contribute to the technological advancement of wind-assisted propulsion systems, and support their broader application in real-world maritime operations in alignment with the IMO decarbonization goals.

2. Numerical Analysis

2.1 Computational Conditions

This study adopted a crescent-shaped airfoil model based on the baseline geometry commonly used in conventional wing sail designs. Numerical simulations were performed by systematically varying the camber and thickness to investigate their effects on the aerodynamic performance. In particular, this study aimed to quantitatively evaluate the influence of these geometric variations on the lift and thrust characteristics, thereby providing foundational data for improving wing sail system performance.

The computational domain was configured with the distance from the inlet boundary to the leading edge of the airfoil set to 20 times the chord length, ensuring stable inflow conditions and minimizing the influence of the boundary on the simulation results. In the downstream direction, the domain was extended to 24 times the chord length to accurately capture the wake structures and flow separation behind the airfoil.

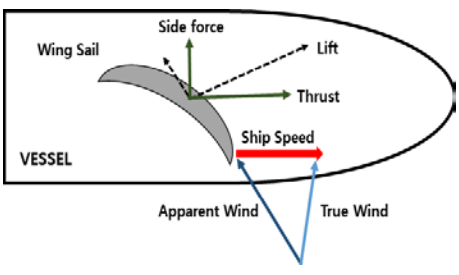

Figure 1: Force components acting on wing sail

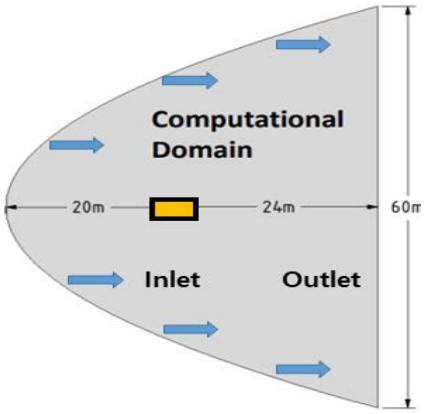

Figure 2: Computational domain and boundary conditions

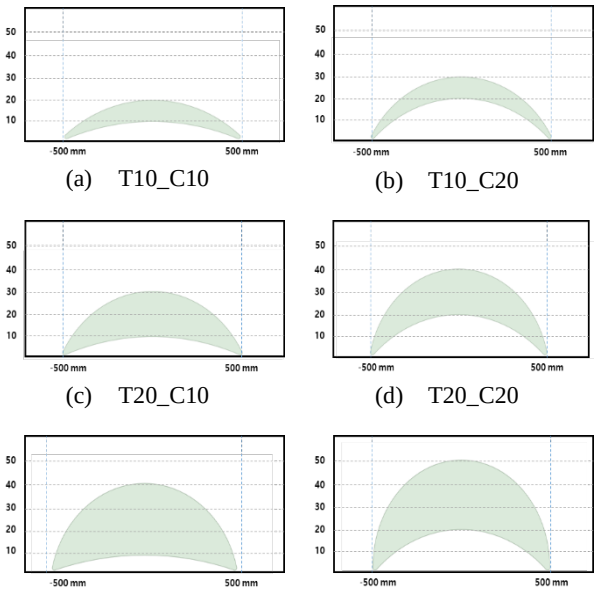

Figure 3: Crescent-shaped airfoil geometry with variations in th ickness and camber

This domain setup plays a crucial role in ensuring the accuracy and convergence stability of the numerical analysis. The detailed computational setup and boundary conditions used in this study are shown in **Figure 2**. Velocity inlet, pressure outlet, and no-slip conditions were applied to the solid walls. These conditions were meticulously designed to realistically reproduce flow characteristics under actual marine conditions.

Figure 3 shows the various crescent-shaped airfoil geometries used in the simulations, showing the configurations generated by systematically varying the thickness and camber length. The thickness was set in the range of 10%–30% of the chord length (1000 mm), and the camber was varied between 10% and 20%. These configurations were specifically designed to assess

the effects of thickness and camber variations on the lift and thrust characteristics.

Domain configuration is crucial in ensuring the accuracy and convergence stability of numerical analysis. The detailed numerical setup and boundary conditions used in this study are presented in **Figure 2**. These include the velocity inlet, pressure outlet, and no-slip boundary conditions applied to the solid walls. Such settings were carefully chosen to realistically replicate the flow behavior under real sea conditions, thereby enabling the precise characterization of the flow field around the airfoil.

2.2 Computational Grid

To evaluate the thrust generated by the crescent-shaped airfoil, CFD analysis was conducted using the commercial software Ansys Fluent V2022R2.

For turbulence modeling, the k–ω shear stress transport (SST) model was employed, as it is well-suited for accurately capturing viscous flow behavior within the boundary layer near the wall **[14]**. This model is particularly effective for predicting complex boundary layer phenomena, such as flow separation and reattachment, making it appropriate for achieving the objectives of this study.

The mesh was generated with consideration for both numerical accuracy and computational efficiency. It was created using Ansys Mesh, an automated meshing tool that is robust and reliable for preprocessing complex geometries. To represent the curved surface of the crescent-shaped airfoil accurately, a tetrahedral mesh structure composed of triangular elements was adopted, ensuring high mesh quality suitable for resolving intricate geometries.

To enhance the convergence and simulation accuracy, local mesh refinement was applied near the airfoil surface, particularly in regions that directly interact with wall-bounded flow. In these near-wall regions, high-resolution meshes were used to capture the boundary-layer development, flow separation, and vortex formation. The dimensionless wall distance (y^+) was maintained below 1 to enable direct resolution of the boundary layer without relying on wall functions. The total number of mesh elements was approximately 300,000, with slight variations depending on the y^+ condition. The final mesh distribution, as shown in **Figure 4**, demonstrated an overall uniform structure and acceptable aspect ratios. The mesh quality was thoroughly assessed to minimize skewed or distorted elements that could lead to numerical instability.

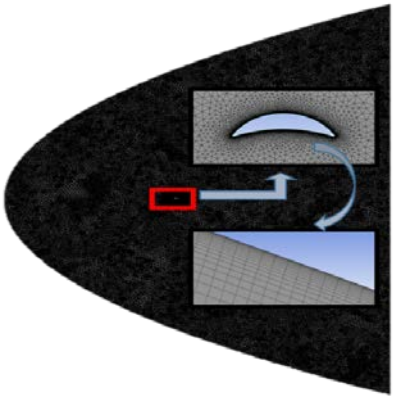

Figure 4: Computational grid around the crescent-shaped airfoil

3. Results and Discussion

To ensure the reliability of the CFD analysis, this study validated the numerical results obtained from Fluent against the aerodynamic experimental data obtained by Abbott at NASA **[15]**. The validation focused on the variations in the lift coefficient (C_L) and drag coefficient (C_D), with respect to the angle of attack, as shown in **Figure 5**. The Fluent results demonstrated an overall good agreement with the experimental data, with negligible discrepancies observed before stall onset. The general trend was accurately reproduced even beyond the stall angle, confirming the reliability of the Fluent-based simulation environment used in this study. Based on the validated setup, a full-scale numerical analysis of a crescent-shaped wing sail was conducted.

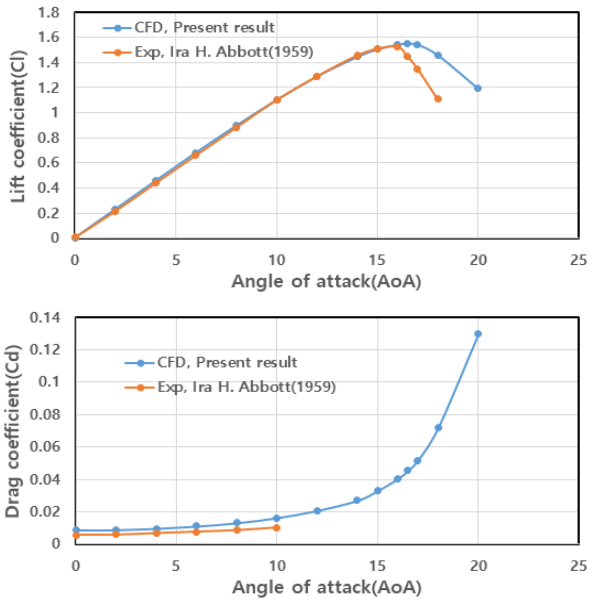

Figure 5: Cross-validation of CFD and experimental data

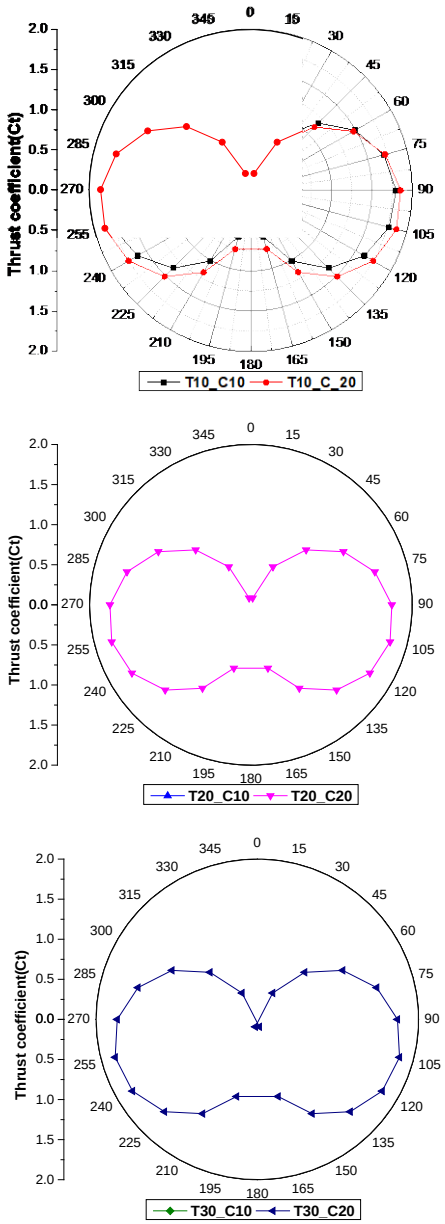

Figure 6: Variation of thrust coefficient with camber change

Figure 6 shows the thrust coefficient (Ct) distribution in polar coordinates for different camber values under fixed thickness conditions. Under the 10% thickness condition (T10), Ct increased significantly as the camber changed from C10 to C20, and the sensitivity to the wind direction also became more pronounced. This result is interpreted as the effect of the increased curvature in thin airfoils, which leads to closer adherence of the flow along the surface and improved pressure distribution, thereby enhancing thrust. Under the 20% thickness configuration (T20), a generally stable Ct distribution was observed, although the improvement owing to the increased camber was slightly less pronounced compared to T10. This indicates that the combination of thickness and camber plays a key role in optimizing wing sail performance.

In contrast, under the 30% thickness configuration (T30), the variation in Ct with respect to wind direction was less significant than that in T10 and T20, and all three cases showed similar overall patterns. This can be attributed to the increased boundary layer development, flow separation, and vortex formation caused by the increased thickness, which degrades the aerodynamic performance. In other words, as the thickness increased, the effect of the camber diminished, and the aerodynamic benefits of the increased curvature were offset by the increase in drag. These results demonstrate that the effect of camber variation is more pronounced in thinner airfoils and that maintaining a thin profile with a higher camber is advantageous for maximizing thrust performance. This finding highlights an important geometric design criterion for crescent-shaped wing sails.

Figure 7 shows how Ct varies with changes in thickness while camber is kept constant. Two cases were examined: camber fixed at 10% and 20%, with thicknesses varying from 10%, 20%, and 30% across wind directions ranging from 0° to 180°. Under the 10% camber condition (C10), all the thickness combinations exhibited a generally circular distribution. The maximum

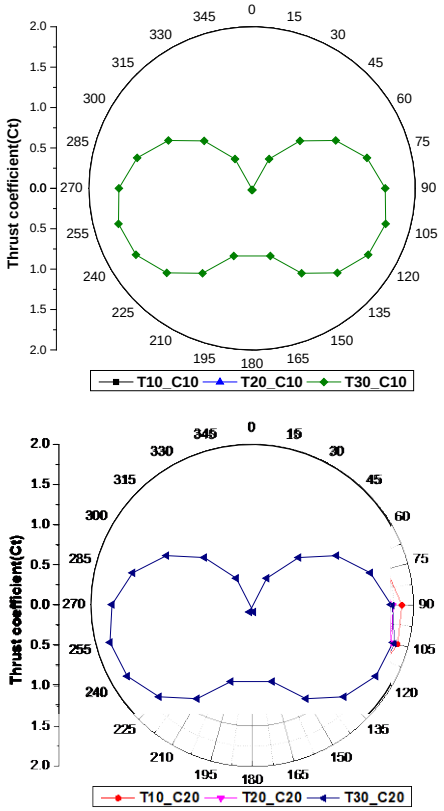

Figure 7: Variation in thrust coefficient with thickness change

Ct values were observed at approximately 90° and 270°, whereas the minimum values were observed at 0° and 180°. As the thickness increased, the absolute Ct values tended to decrease, with T10 generally exhibiting higher thrust coefficients than T30 across most wind directions. However, for wind directions above 120°, thicker airfoils began to generate higher Ct values, indicating a reverse trend under certain conditions.

Figure 8 compares the overall Ct distributions across the six geometric combinations (three thickness levels × two camber levels). The results showed that the T10_C20 configuration achieved the highest Ct across all wind directions, indicating the best aerodynamic performance, whereas T30_C10 consistently showed the lowest performance. These findings indicate that a thin, highly cambered profile is most effective for improving thrust, demonstrating that the combination of thickness and camber is a critical parameter in wing sail design.

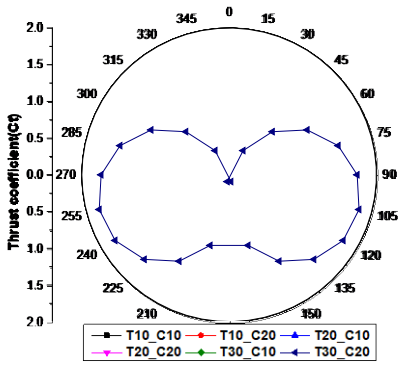

Figure: 8 Variation in thrust coefficient with change in camber and thickness

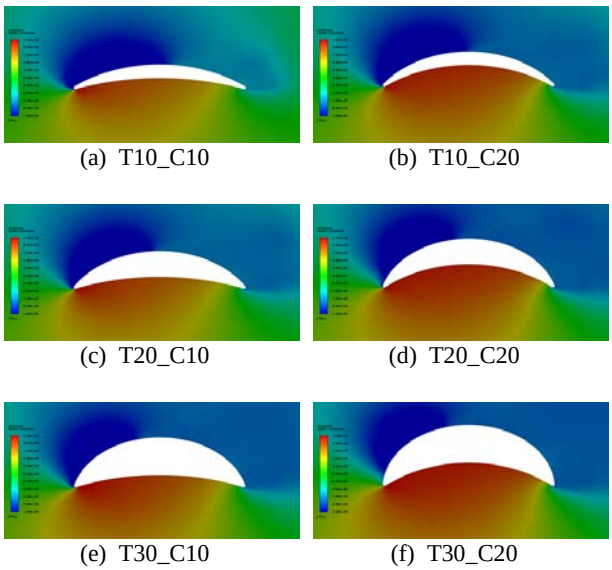

(a) T10_C10 (b) T10_C20

(c) T20_C10 (d) T20_C20

(e) T30_C10 (f) T30_C20

Figure 9: Distribution of pressure around wing sail

Figure 9 illustrates the pressure distribution patterns resulting from different camber and thickness combinations. The simulations were conducted under the same angle of attack, and the resulting pressure contours served as key indicators for evaluating aerodynamic performance. As the thickness decreased and camber increased, a broader and stronger low-pressure region formed on the upper surface of the airfoil, resulting in improved lift and thrust. This observation was consistent with the Ct distribution analysis.

Figure 10 shows the effects of camber and thickness on the lift coefficient (C_L) and drag coefficient (C_D). The first graph clearly shows that both C_L and C_D increase with the camber. Specifically, for the same thickness, a larger camber produces a greater pressure difference between the upper and lower surfaces, leading to a higher lift but also an increase in drag, reflecting typical aerodynamic behavior. The second graph reveals that as the thickness increases, C_L tends to decrease, whereas C_D increases. This is attributed to earlier flow separation and greater form drag in the thicker profiles. In the third graph, the stall angle increases progressively with increasing thickness and camber, with the T30_C20 configuration exhibiting the highest stall angle.

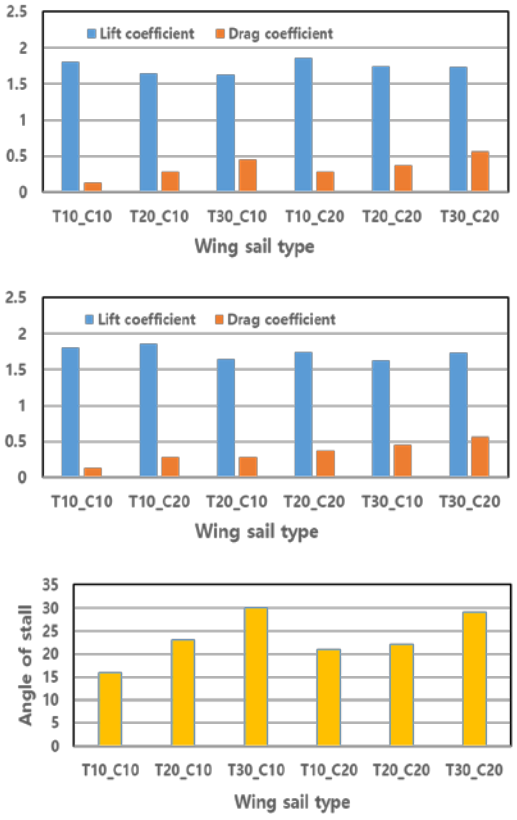

Figure 10: Lift, drag, and stall angle distribution according to thickness and camber

4. Conclusion

This study entailed a CFD-based numerical analysis of crescent-shaped airfoils to enhance the performance of wing sails, a representative eco-friendly marine propulsion technology in response to IMO environmental regulations. The effects of camber and thickness combinations on the thrust coefficient (Ct) were quantitatively analyzed to provide foundational data for optimizing the wing sail design.

The thrust performance was evaluated under omnidirectional wind conditions (0°–360°) for six geometric configurations (T10_C10–T30_C20). The configuration with the thinnest profile and largest camber (T10_C20) demonstrated the highest overall Ct values. This is attributed to the favorable pressure distributions generated by the close adherence of the flow along the curved surface, which significantly contributes to thrust enhancement.

In contrast, as the airfoil thickness increased, the performance difference owing to camber variation gradually diminished. Specifically, under the 30% thickness configuration, the effect of the camber became less significant. This phenomenon is attributed to the increased boundary layer development and flow separation in thicker profiles, which leads to greater flow instability and drag.

The pressure distribution analysis further supports these findings. Thin, highly cambered airfoils form wider and stronger low-pressure regions on the upper surface, resulting in superior aerodynamic performance, whereas thicker profiles exhibit relatively weaker pressure differentials and degraded performance. In addition, as the number of cameras increased, both the lift and drag coefficients increased. With increasing thickness, the lift decreased and the drag increased, in alignment with typical aerodynamic behavior. The stall angle was also found to increase progressively with the camber and thickness.

In conclusion, the combination of a thin airfoil and a large camber was shown to be the most effective design condition for improving the propulsion performance of crescent-shaped wing sails. The T10_C20 configuration, in particular, emerged as an optimal design candidate, offering both high thrust efficiency and operational stability.

These results may contribute to fuel savings and GHG reduction and can serve as a foundational reference for the design of wing sails applicable to various ship types and routes. Future research should include integrated design approaches that encompass structural stability, manufacturability, and full-scale sea trials.

Acknowledgement

This work was supported by the Ministry of Trade, Industry and Energy (MOTIE, Korea)'s research and development (2025-02634493, development and demonstration of wing sails for LNG carriers with power saving effect of 300 kW or higher).

Author Contributions

Conceptualization, Methodology, Software, Formal Analysis, Investigation, Resources, Data Curation, Writing-Original Draft Preparation, Writing-Review & Editing, Visualization, Supervision, Project Administration, Funding Acquisition, J. H. Kim.

References

[1] IMO, Fourth IMO GHG Study 2020, International Mari time Organization, 2020.

[2] IMO, MEPC.328(76): Amendments to MARPOL Annex VI – EEXI and CII, International Maritime Organization, 2021.

[3] ICCT, Global shipping GHG emissions 2013–2015, https://theicct.org/wp-content/uploads/2021/06/Global-shipping-GHG-emissions-2013-2015_ICCT-Report_17102017_vF.pdf, Accessed June 8, 2025.

[4] E. Czermanski, A. Oniszczuk-Jastrząbek, E. F. Spangenberg, Ł. Kozłowski, M. Adamowicz, J. Jankiewicz, G. T. Cirella, “Implementation of the energy efficiency existing ship index: an important but costly step towards ocean protection,” Ocean Engineering, vol. 145, 105259, 2022.

[5] A. Sardar, R. Islam, M. Anantharaman, V. Garaniya, “Advancements and obstacles in improving the energy efficiency of maritime vessels: A systematic review,” Marine Pollution Bulletin, vol. 214, 117688, 2025.

[6] F. Thies and J. W. Ringsberg, “Wind-assisted, electric, and pure wind propulsion – the path towards zero-emission RoRo ships,” Ships and Offshore Structures, vol. 18, no. 8, pp. 1229-1236, 2023.

[7] M. Traut, P. Gilbert, C. Walsh, A. Bows, and *et al.*, “Propulsive power contribution of a kite and a Flettner rotor on selected shipping routes,” Applied Energy, vol. 113, pp. 362-372, 2014.

[8] K. Hochkirch and V. Bertram, “Wind assisted propulsion: Economic and ecological considerations,” Maritime Technology and Research, vol. 4 no. 3, 2022.

[9] S. -D. Kim., S. J. Yun, and J. H. Kim “Study on physical modeling and simulation of a maritime substantiation vessel for verifying the operational efficiency of a rotor sail,” Journal of Advanced Marine Engineering and Technology, vol. 48, no. 6, pp. 480-486, 2024.

[10] H. J. Lee, Y. M. Cho, H. I. Kwon, and S.I. Choi, “Aerodynamic design optimization of wing-sails in consideration of the flow interactions,” the Korean Society for Computational Fluids Engineering, 2013 Summer Conference, p. 223-233, 2013.

[11] R. Ma, Q. Zhao, K. Wang, J. Cao, C. Yang, Z. Hu, and L. Huang, “Energy efficiency improvement technologies for ship in operation: A comprehensive review” Ocean Engineering, vol. 331, 121258, 2025.

[12] C. Guzelbulut, T. Badalotti, K. Suzuki, “Optimization techniques for the design of crescent-shaped hard sails for wind-assisted ship propulsion,” Ocean Engineering, vol. 312, 119142, 2024.

[13] H. Yao, F. Thies, J. W. Ringsberg, and B. Ramne, “Propulsive performance of a rigid wingsail with crescent-shaped profiles,” Ocean Engineering, vol. 285, 115349, 2023.

[14] ANSYS, ANSYS Fluent User's Guide, 2022R2.

[15] H. Abbott and A. E. von Doenhoff, Theory of Wing Sections: Including a Summary of Airfoil Data, New York, USA: Dover Publications, p. 462, 1959.